Stabilization of Strontium Analogues of Barium Yttrium Cuprate Perovskites via Chemical Substitution

S. A. Sunshine,* L. F. Schneemeyer, T. Siegrist, D. C. Douglass, J. V. Waszczak, R. J. Cava, E. M. Gyorgy, and D. W. Murphy

AT&T Bell Laboratories, 600 Mountain Avenue, Murray Hill, New Jersey 07974

Received January 3, 1989

We report the synthesis and characterization of $Sr_2YCu_{3-x}M_xO_y$, M = Al, Pb, Fe, and Co, analogues of the 92 K superconducting perovskite $Ba_2YCu_3O_7$. While phase-pure $Sr_2YCu_3O_7$ cannot be prepared, cation substitution for Cu stabilizes this phase. Crystals of these phases were grown from CuO-rich melts containing appropriate melt impurities or from lead oxide based melts. Ceramic samples were prepared for detailed studies of stability ranges, oxygen content, and property/dopant relationships. For $Sr_2YCu_{3-x}M_xO_{7+\delta}$, samples with M = Al or Co have $\delta = 0$ for all x and $\delta > 0$ when M = Fe and $x \approx 1$. Samples were characterized by resistivity and dc magnetic susceptibility measurements. Superconductivity is observed in samples with low levels of metal substitution; however, the volume fraction is small (<2%) and cannot be uniquely attributed to the perovskite phase. A comparison of solid-state ^{27}Al NMR spectra of Ba- and Sr-based perovskites suggest a different Al environment in these two systems.

Introduction

Since the discovery of superconductivity above 77 K in $Ba_2YCu_3O_7$[1,2] a myriad of chemical substitutions have been reported. Almost all rare-earth metals can replace Y with little change in T_c.[3-7] The copper in both the chain and plane sites (Figure 1) has been substituted by other metal ions.[8-20] The exact location of the substituted metals has been analyzed by Mossbauer and Raman spectroscopy as well as by X-ray and neutron diffraction. There is general agreement between researchers that at low levels of substitution Co, Fe, and Al substitute on the chain sites[8,21] while Ni and Zn substitute onto the planes.[8,21] Such substitutions lower T_c dramatically.[8,13,15,17] While Sr substitution for Ba has been reported,[22-27] there are con-

Table I. Crystal Growth Parameters and Results

flux comp	crucible	T_{max}, °C	cooling rate, °C/h	product
$Sr_4YCu_{10}O_x$	Al_2O_3	1050	3–10	$Sr_2YCu_{3-x}Al_xO_{7-\delta}$
$Sr_4YCu_{10}O_x$	ZrO_2	1050	3–10	$(Sr,Y)_{14}Cu_{24}O_{41}$[32,33]
$Sr_4YCu_{10}Fe_{0.1}O_x$	ZrO_2	1050	8	$Sr_2YCu_{3-x}Fe_xO_{7-6}$
$SrYPb_4Cu_2O_x$	Al_2O_3	1000	10	$Sr_2YCu_{3-x}Pb_xO_{7-\delta}$

Table II. Summary of Data Aquisition Parameters for $Sr_2YCu_{3-x}M_xO_{7+\delta}$

	M = Al	M = Pb
x	0.67	0.61
space group	$P4/mmm$	$P4/mmm$
a, Å	3.814 (1)	3.832 (1)
c, Å	11.303 (2)	11.902 (5)
vol, Å^3	164.4	174.8
Z	1	1
cryst vol, mm^3	0.22 × 0.24 × 0.11	0.08 × 0.06 × 0.01
cryst shape	platelet	platelet
ρ_{calcd}, g cm^{-3}	5.64	6.07
linear abs coeff, mm^{-1}	32.0	41.2
scan type	ω–2θ	ω
$\lambda^{-1} \sin\theta$, limits	0.0615–0.7049	0.0615–0.7049
data coll	1634	483
unique data	263	279
data with $F_o > 2\sigma F_o$	217	189
no. of variables	21	17
$R(F)$	0.067	0.108
$R(F_w)$	0.065	0.080
$R(F)$ for $F_o > 2\sigma F_o$	0.057	0.078

(1) Wu, M. K.; Ashburn, J. R.; Torng, C. T.; Hor, P. H.; Meng, R. L.; Gao, L.; Huang, Z. J.; Wang, Y. Q.; Chu, C. W. *Phys. Rev. Lett.* **1987**, *58*, 908.
(2) Cava, R. J.; Batlogg, B.; van Dover, R. B.; Murphy, D. W.; Sunshine, S.; Siegrist, T.; Remeika, J. P.; Rietman, E. A.; Zahurak, S.; Espinosa, G. P. *Phys. Rev. Lett.* **1987**, *58*, 1676.
(3) Hor, P. H.; Meng, R. L.; Wang, Y. Q.; Gao, L.; Huang, Z. J.; Bechtold, J.; Forster, K.; Chu, C. W. *Phys. Rev. Lett.* **1987**, *58*, 1891.
(4) Schneemeyer, L. F.; Waszczak, J. V.; Zahurak, S. M.; van Dover, R. B.; Siegrist, T. *Mater. Res. Bull.* **1987**, *22*, 1467.
(5) Tarascon, J. M.; McKinnon, W. R.; Greene, L. H.; Hull, G. W.; Vogel, E. M. *Phys. Rev. B: Condens. Matter* **1987**, *36*, 8393.
(6) Willis, J. O.; Fisk, Z.; Thompson, J. D.; Cheong, S.-W.; Aikin, R. M.; Smith, J. L.; Zirngiebl, E. *J. Magn. Magn. Mater.* **1987**, *L139*, 67.
(7) Kishio, K.; Kitizawa, K.; Sugii, N.; Kanabe, S.; Fueki, K.; Takagi, H.; Tanaka, S. *Chem. Lett.* **1987**, 635.
(8) Tarascon, J. M.; Barboux, P.; Miceli, P. F.; Greene, L. H.; Hull, G. W.; Eibschuttz, M.; Sunshine, S. A. *Phys. Rev. B: Condens. Matter* **1988**, *37*, 7459.
(9) Maeno, Y.; Tomita, T.; Kyogoku, M.; Awaji, S.; Oki, Y. A.; Hoshino, K.; Minami, A. A.; Fujita, T. *Nature* **1987**, *328*, 512.
(10) Maeno, Y.; Kato, M.; Aoki, Y.; Fujita, T. *Jpn. J. Appl. Phys.* **1987**, *26*, L1982.
(11) Boolchand, P.; Blue, C.; Elgaid, K.; Zitkovsky, I.; McDaniel, D.; Huff, W.; Goodman, B.; Lemon, G.; Farrell, D. E.; Chandrasekhar, B. S. *Phys. Rev. B: Condens. Matter* **1988**, *38*, 11313.
(12) Bottyan, L.; Molnar, B.; Nagy, D. L.; Sxucs, I. S.; Toth, J.; Dengler, J.; Ritter, G.; Schober, J. *Phys. Rev. B: Condens. Matter* **1988**, *38*, 11373.
(13) Bringley, J. F.; Chen, T.-M.; Averill, B. A.; Wong, K. M.; Poon, S. J. *Phys. Rev. B: Condens. Matter* **1988**, *38*, 2432.
(14) Zolliker, P.; Cox, D. E.; Tranquanda, J. M.; Shirane, G. *Phys. Rev. B: Condens. Matter* **1988**, *30*, 6575.
(15) Xiao, G.; Cieplak, M. Z.; Musser, D.; Gavrin, A.; Streitz, F. H.; Chien, C. L.; Rhyne, J. J.; Gotaas, J. A. *Nature* **1988**, *332*, 238.
(16) Tang, H.; Qiu, Z. Q.; Du, Y.-W.; Xiao, G.; Chien, C. L.; Walker, J. C. *Phys. Rev. B: Condens. Matter* **1987**, *36*, 4018.
(17) Takabatake, T.; Ishikawa, M. *Solid State Commun.* **1988**, *66*, 413.
(18) Kajitani, T.; Kusaba, K.; Kiruchi, M.; Syono, Y.; Hirabayashi, M. *Jpn. J. Appl. Phys.* **1988**, *27*, L354.
(19) Tamaki, T.; Komai, T.; Ito, A.; Maeno, Y.; Fujita, T. *Solid State Commun.* **1988**, *65*, 43.
(20) Iqbal, Z.; Steinhauser, S. W.; Bose, A.; Cipollini, N.; Eckhardt, H. *Phys. Rev. B: Condens. Matter* **1987**, *36*, 2283.
(21) Kistenmacher, T. *Phys. Rev. B: Condens. Matter* **1988**, *38*, 8862.
(22) Ono, A.; Tanaka, T.; Nozaki, H.; Ishizawa, Y. *Jpn. J. Appl. Phys.* **1987**, *26*, L1687.
(23) Veal, B. W.; Kwok, W. K.; Umezawa, A.; Crabtree, G. W.; Jorgensen, J. D.; Downey, J. W.; Nowicki, L. J.; Mitchell, A. W.; Paulikas, A. P.; Sower, C. H. *Appl. Phys. Lett.* **1987**, *51*, 279.
(24) Khan, Y. *J. Mater. Sci. Lett.* **1988**, *7*, 374.
(25) Oda, M.; Murakami, T.; Enomoto, Y.; Suzuki, M. *Jpn. J. Appl. Phys.* **1987**, *26*, L804.
(26) Wu, M. K.; Ashburn, J. R.; Higgins, C. A.; Loo, B. H.; Burns, D. H.; Ibrahim, A.; Rollins, T. D.; Chien, F. Z.; Huang, C. Y. *Phys. Rev. B: Condens. Matter* **1988**, *B37*, 9765.

0897-4756/89/2801-0331$01.50/0

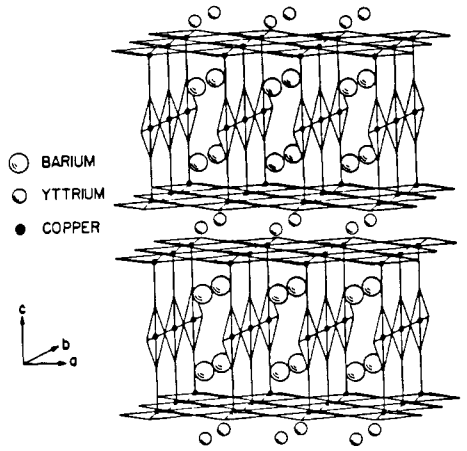

Figure 1. Structure of $Ba_2YCu_3O_7$ showing Cu–O chains and planes.

flicting data as to the extent of the solid solution $Ba_{2-y}Sr_yYCu_3O_{7-\delta}$. The synthesis of pure $Sr_2YCu_3O_7$ has been claimed,[25-27] although others report that the solid solution extends only to $Ba_{0.8}Sr_{1.2}YCu_3O_{7-\delta}$.[22-24] We have been unable to prepare $Sr_2YCu_3O_7$, but we have found that the phase is stabilized by a variety of metal ions substituted for copper. In this paper, we report the preparation of perovskite phases of the formula $Sr_2YCu_{3-x}M_xO_7$, where M = Al, Fe, Co, and Pb, as both ceramics and single crystals. The synthesis of a similar phase in the Sr–Y–Pb–Ca–Cu–O system has recently been reported.[28] We show that metals substituting on the Cu chain sites can stabilize the perovskite phase and that at low levels of metal incorporation the samples are superconductors. The physical properties and oxygen stoichiometry of these materials are discussed.

Experimental Section

Crystals were grown from copper oxide rich fluxes similar to those employed in the growth of $Ba_2YCu_3O_7$.[29] Strontium cuprate–copper oxide based melts melt somewhat higher than the barium analogues. Melt compositions and growth conditions are listed in Table I. Copper oxide, strontium carbonate, and yttrium oxide mixtures plus the appropriate metal oxide were ground together and placed in high-density Al_2O_3 or ZrO_2 crucibles. Samples were rapidly heated to T_{max}, then slow cooled at rates of 5–25 °C/h to a temperature below the temperature of melt solidification, here ≈950 °C. Ceramic samples were prepared by standard ceramic techniques using $Ba(NO_3)_2$, CuO, Y_2O_3, PbO, $CoCO_3$, NiO, Fe_2O_3, $ZnCO_3$, and $Al(NO_3)_3 \cdot 9H_2O$ as starting materials. Typical sample preparation involved several cycles of grinding and firing at 950–1050 °C with a final anneal in flowing O_2 at 500 °C.

Single-crystal X-ray diffraction data were collected on an Enraf-Nonius CAD4 diffractometer with graphite-monochromated Mo Kα radiation. All subsequent calculations were carried out using the NRCVAX structure package.[30] An analytical absorption correction was applied, and equivalent reflections were averaged. Details of data collection and analysis parameters are given in Table II.

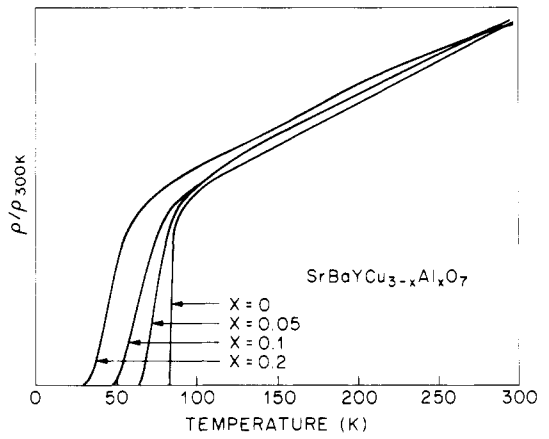

Figure 2. Temperature dependence of the resistivity normalized to the room-temperature value for samples in the series $SrBaYCu_{3-x}Al_xO_7$.

The solid-state ^{27}Al NMR spectra were obtained in a 7.05-T field (78.2 MHz) at room temperature by using a 90_x–τ–180_x spin-echo pulse sequence for the $^1/_2 \leftrightarrow {}^{-1}/_2$ transition; the 90° pulse length is ≈2μ and τ is 20μ. The spectrum of the $^1/_2 \leftrightarrow {}^3/_2$ and the $^{-1}/_2 \leftrightarrow {}^3/_2$ transitions were observed in a large sample of composition $Sr_2YCu_2AlO_7$ by stepping through a frequency range of 2.5 MHz with a narrow-band excitation.

Thermal gravimetric analysis studies were carried out by using a Du Pont Model 1090 analyzer. Oxidation-state titrations were performed by dissolving the sample in an acidified solution of KI and back titration of the iodine formed.[31] Resistivity measurements were made in either van der Pauw or four-point configuration using an ac constant-current source and phase-sensitive detection.

Results

Conflicting reports as to the range of the solid solution in $Ba_{2-y}Sr_yYCu_3O_7$ have some researchers claiming that this solid solution extends to $Sr_2YCu_3O_7$[25-27] while others find that $0 \leq y \leq 1.2$.[22,23] In investigating the $Ba_{2-y}Sr_yYCu_3O_7$ system, we find that the solid solution extends only to $y = 1.2$, in agreement with other workers.[22,23] Our attempts to prepare $Sr_2YCu_3O_7$ yielded instead a new phase in the Sr–Y–Cu–O system; $(Sr,Y)_{14}Cu_{24}O_{41}$, a layered structure type containing distorted Cu–O chains and planes.[32,33] During crystal growth in alumina crucibles a second new phase containing Sr–Y–Cu–O was isolated. Energy-dispersive X-ray analysis indicated the presence of Al in these samples, and X-ray diffraction studies suggested a cell similar to $Ba_2YCu_3O_7$ ($a = b = 3.84$, $c = 11.28$ Å).

To gain insight into the role of metal substitution in the stabilization of Sr perovskites, the system $Ba_{2-y}Sr_yYCu_{3-x}Al_xO_7$ was investigated. We find that as y increases beyond 1.2, the addition of Al will stabilize the perovskite structure. At $x = 0.4$ the perovskite structure is stable to $y = 2$. A detailed look at the system $BaSrYCu_{3-x}Al_xO_7$ indicates that increasing x reduces T_c and broadens the superconducting transition. Figure 2 shows the resistivity as a function of temperature for several samples in this series.

In addition to aluminum, we have found other metals that stabilize the tripled perovskite structure of $Sr_2YCu_3O_7$. To date, compounds of composition $Sr_2YCu_{3-x}M_xO_7$ with

(27) Qi-rui, Z.; Lie-zhao, C.; Yi-tai, Q.; Zu-yao, C.; Wei-yan, G.; Yong, Z.; Guo-gang, P.; Han, Z.; Jian-sheng, X.; Ming-Jian, Z.; Dao-qi, Y.; Zheng-hui, H.; Shi-fang, S.; Ming-hu, F.; Tao, Z. *Solid State Commun.* **1987**, *63*, 535.

(28) Subramanian, M. A.; Gopalakroshnan, J.; Torardi, C. C.; Gai, P. L.; Boyes, E. D.; Askew, T. R.; Flippen, R. P.; Farneth, W. E.; Sleight, A. W. *Physica C* **1989**, *157*, 124.

(29) Schneemeyer, L. F.; Waszczak, J. V.; Siegrist, T.; van Dover, R. B.; Rupp, L. W.; Batlogg, B.; Cava, R. J.; Murphy, D. W. *Nature* **1987**, *328*, 601.

(30) Gabe, E. J.; Lee, F. C.; LePage, Y. *Crystallographic Computing 3*; Sheldrick, G. H., Kruger, C. H., Goddard, R., Eds.; Clarendon: Oxford, 1985; p 163.

(31) Demazeau, G.; Marty, J. L.; Buffat, B.; Dance, J. M.; Pouchard, M.; Dordor, P.; Chevalier, B. *Mater. Res. Bull.* **1982**, *17*, 37.

(32) Siegrist, T.; Schneemeyer, L. F.; Sunshine, S. A.; Waszczak, J. V.; Roth, R. S. *Mater. Res. Bull.* **1988**, *23*, 1429.

(33) McCarron, E. M.; Subramanian, M. A.; Calabrese, J. C.; Harlow, R. L. *Mater. Res. Bull.* **1988**, *23*, 1355.

Table III. Crystallographic Data for $Sr_2YCu_{2.33}Al_{0.67}O_{6.63}$[a]

atom	x	y	z	B_{iso}, Å^2	occupancy
Sr	1/2	1/2	0.1926 (2)	1.66 (5)	
Y	1/2	1/2	1/2	0.80 (5)	
Cu(1)	0	0	0	3.19 (20)	0.33 (4)
Al	0	0	0	3.19 (20)	0.67 (4)
Cu(2)	0	0	0.3508 (2)	0.88 (10)	
O(1)	0	0	0.151 (2)	4.2 (7)	
O(2)	1/2	0	0.3727 (9)	1.3 (3)	
O(3)	0	1/2	0	10.4 (60)	0.63 (6)

[a] Tetragonal lattice (oxygen annealed), space group $P4/mmm$, a = 3.814 (1) Å, c = 11.303 (2) Å, Z = 1; 1634 reflections measured, 263 unique, R_F = 0.067. The estimated standard deviations (in parentheses) refer to the last digit printed.

Table IV. Crystallographic Data for $Sr_2YCu_{2.39}Pb_{0.61}O_6$[a]

atom	x	y	z	B_{iso}, Å^2	occupancy
Sr	1/2	1/2	0.2084 (3)	0.92 (9)	
Y	1/2	1/2	1/2	0.4 (1)	
Cu(1)	0	0	0	2.4 (1)	0.39 (5)
Pb	0	0	0	2.4 (1)	0.61 (5)
Cu(2)	0	0	0.3599 (4)	0.5 (1)	
O(1)	0	0	0.166 (4)	2.9 (8)	
O(2)	1/2	0	0.374 (2)	0.8 (3)	

[a] Tetragonal lattice (as grown), space group $P4/mmm$, a = 3.832 (1) Å, c = 11.902 (5) Å, Z = 1; 483 reflections measured, 279 unique, R_F = 0.11.

M = Pb, Co, Fe, and Al have been prepared as single crystals or as bulk ceramics. The effects of metal substitution on the crystal growth, lattice parameters, oxygen stoichiometry, and physical properties of strontium cuprate perovskites has been investigated.

Crystal Growth and Structure. Crystals of Pb-, Fe-, and Al-doped samples have been grown from CuO-rich melts containing appropriate melt impurities or from lead oxide based melts. The conditions and results of several crystal growth experiments are summarized in Table I. For Pb and Al samples, single-crystal X-ray diffraction studies indicate the same metal atom arrangement as $Ba_2YCu_3O_7$ with Pb or Al substituting for the chain copper atoms (Figure 1). Unfortunately, the X-ray experiment is not sensitive to the placement of oxygen atoms around the substituted metals or to the possibility of Sr–Y site disorder. The former is due in part to a high degree of correlation between the occupancy of O(3) and M sites. In the case of Pb, addition of electron density at O(3) resulted in a large thermal parameter for this site and no improvement in the overall refinement. This refinement is in general agreement with an isostructural compound in the Sr–Y–Ca–Pb–Cu–O system[28] as concerns the metal atom positions. Single-wavelength X-ray experiments are also unable to differentiate between Fe or Co and Cu, although by analogy with the $Ba_2YCu_3O_7$ system[8,21] we assume they also occupy the chain copper site. The results of the X-ray refinements for Pb- and Al-containing crystals are given in Tables III and IV.

Lattice Parameters. In ceramic samples, the strontium yttrium cuprate perovskite $Sr_2YCu_{3-x}M_xO_7$ is found to be stable for M = Al, Co, Fe, and Pb. Lattice parameters for single-phase samples were determined by least-squares refinement of at least 10 reflections between 5 and 65° 2θ (Cu Kα). A summary of the lattice parameters for these samples is given in Table V. Attempts to prepare Zn- and Ni-substituted samples have been unsuccessful. For Al, single-phase ceramic samples of composition $Sr_2YCu_{3-x}Al_xO_7$, $0.4 \le x \le 1.0$, have been prepared. Attempts to prepare samples with smaller values of x result in multiphase samples as determined by X-ray powder diffraction. All samples exhibit tetragonal symmetry with

Table V. Lattice Parameter, Stoichiometry, and Resistivity Data for $Sr_2YCu_{3-x}M_xO_{7+\delta}$

M	x	a, Å	c, Å	V	δ[a]	ρ_{rt}, Ω cm
Al	0.4	3.830 (3)	11.344 (8)	166.4	−0.12[r]	0.059
	0.5	3.832 (2)	11.316 (7)	166.1	−0.08[r]	0.040
	0.6	3.842 (3)	11.298 (8)	166.8	−0.03[t]	0.055
	0.7	3.848 (2)	11.279 (5)	167.0	−0.04[r]	0.099
	0.8	3.851 (2)	11.242 (6)	166.7	−0.14[r]	0.31
	0.9	3.865 (4)	11.212 (9)	167.5	−0.06[r]	1.20
	1.0	3.867 (2)	11.142 (5)	166.6	0.06[t]	3.75
Fe	0.4	3.806 (1)	11.410 (2)	165.3	−0.28[t]	0.0108
	0.5	3.807 (2)	11.402 (7)	165.3	−0.21[t]	0.0102
	0.6	3.815 (4)	11.376 (11)	165.6	−0.12[t]	0.0277
	0.7	3.827 (4)	11.380 (10)	166.7	−0.05[t]	0.0125
	0.8	3.822 (3)	11.356 (8)	165.9	+0.02[t]	0.0146
	0.9	3.823 (3)	11.363 (9)	166.1	+0.06[t]	0.0709
	1.0	3.826 (3)	11.365 (9)	166.3	+0.12[t]	0.119
Co	0.4	3.820 (3)	11.454 (7)	167.1	−0.23[r]	3.741
	0.5	3.825 (2)	11.472 (5)	167.8	−0.05[r]	0.0281
	0.6	3.833 (2)	11.471 (6)	168.5	−0.07[r]	0.0446
	0.7	3.837 (4)	11.461 (11	168.7	−0.08[r]	0.165
	0.8	3.837 (2)	11.433 (6)	168.3	−0.10[r]	0.764
	0.9	3.844 (3)	11.438 (8)	169.0	−0.06[r]	2.82
	1.0	3.846 (3)	11.426 (9)	169.0	+0.02[r]	35.7
Pb	0.5	3.836 (3)	11.857 (7)	174.5	−0.13[r]	0.262

[a] t, value determined by titration. r, value determined by reduction.

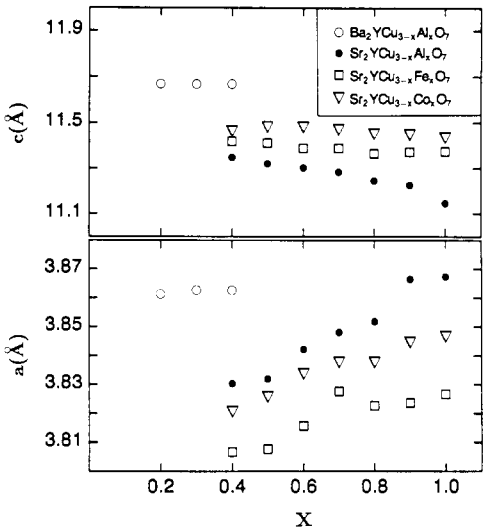

Figure 3. Lattice parameters as a function of composition for samples in the series $Sr_2YCu_{3-x}M_xO_7$, M = Co, Fe, Al. Similar data for $Ba_2YCu_{3-x}Al_xO_7$ (from ref 8) are included for comparison.

a increasing and c decreasing with increasing x as shown in Figure 3. The net result is a very slight increase in cell volume (≈1 Å^3). Solid solutions with M = Fe and Co exhibit similar solid solution limits to the Al system. In general, substitution of at least 40% of the chain site copper is necessary to obtain single-phase perovskite materials, and up to one Cu can be replaced. Small impurity peaks in powder X-ray diffraction experiments are observed if lower dopant levels are attempted, although a large fraction of the perovskite phase if formed. Unlike the Al system, increased Co or Fe substitution causes only a slight decrease in the c parameter, although a significant change in a does occur. The effect is a larger change in cell volume in the case of Co than is observed for Al. At equal levels of substitution (e.g., x = 0.4) the a axis increases in the order Fe < Co < Al. The c axis is shortest when M = Al with Co > Fe (Figure 3). For the larger Pb ion, single-phase samples are obtained only for $0.5 \le x \le 0.7$ where a = 3.836 (3) Å and c = 11.856 (7) Å (Table V). Samples prepared at higher temperatures for longer times

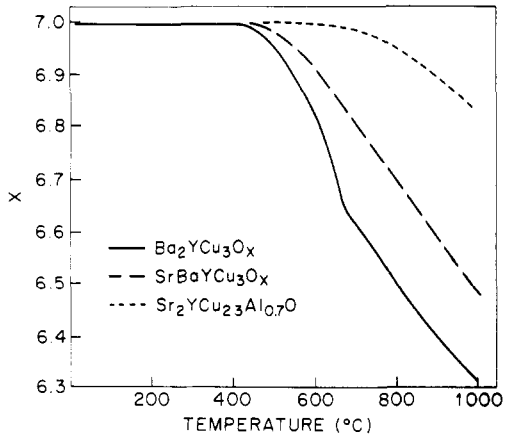

Figure 4. Thermogravametric analysis data for $Ba_2YCu_3O_7$, $SrBaYCu_3O_7$, and $Sr_2YCu_{2.3}Al_{0.7}O_7$ in an O_2 atmosphere.

are single phase at higher dopant levels ($x = 0.7$). Other recent results indicate that the replacement of Y with Ca allows for the stabilization of the perovskite at lower Pb doping.[28] The cell volume for $Sr_2YCu_{3-x}Pb_xO_y$ is actually greater than in $Ba_2YCu_3O_7$.

Oxygen Stoichiometry. Oxygen stoichiometries have been determined by either titration (t) or reduction in H_2/N_2 (r). Previous work on the Ba–Y–Cu–M–O system has shown that the reduction method gives values in good agreement with those obtained in neutron diffraction studies, while the oxidation-state titrations give an underestimate of the oxygen content in heavily doped materials.[8] The oxygen stoichiometries for $Sr_2YCu_{3-x}M_xO_y$ samples determined by these two methods are given in Table V. These samples were heated in flowing oxygen at 500 °C for at least 2 h to ensure maximum oxygen incorporation. For $Sr_2YCu_{3-x}Al_xO_y$ both TGA and oxidation-state titrations indicate that $y \approx 7$ for all compositions. Furthermore, the oxygen variability with temperature is much less than that in $Ba_2YCu_3O_7$. For example, the compound $Sr_2YCu_{2.2}Al_{0.8}O_7$ is stable in N_2 only to $O_{6.9}$, at which point decomposition occurs. In addition, the degree of oxygen loss in an oxygen atmosphere to 1000 °C is very slight. For samples heated to 1000 °C in oxygen, the reversible oxygen loss is greatest for $Ba_2YCu_3O_{7-\delta}$ ($\delta = 0.7$), less for $BaSrYCu_3O_{7-\delta}$ ($\delta = 0.5$), and the least for $Sr_2YCu_{2.3}Al_{0.7-\delta}$ ($\delta = 0.1$) (Figure 4). The degree of oxygen loss in $Ba_2YCu_3O_7$ is also decreased by aluminum substitution.[8] Like the Al samples, heating $Sr_2YCu_2CoO_y$ in oxygen to 950 °C leads to a negligible change in the oxygen content ($y = 6.97$) and reduction indicates that $y \approx 7$ in the fully oxidized material. This is in contrast to $Ba_2YCu_2CoO_y$, where $y \approx 7.4$.[8] Surprisingly, the Fe-substituted samples exhibit a behavior different from the Co- and Al-substituted samples. Oxidation-state titrations indicate a stoichiometry of $Sr_2YCu_2FeO_{7.12}$ in the fully substituted material. When $Sr_2YCu_2FeO_y$ is heated in oxygen, weight loss occurs above 400 °C, and by 1000 °C the oxygen content has been reduced to $y = 6.8$. This behavior is very similar to $Ba_2YCu_2FeO_y$.[8]

Solid-State ^{27}Al NMR Spectroscopy. Figure 5 shows the ^{27}Al NMR spectra of three samples with compositions $Sr_2YCu_2AlO_7$, $Sr_2YCu_{2.4}Al_{0.6}O_7$, and $Ba_2YCu_{2.8}Al_{0.2}O_7$. The spectrum of $Sr_2YCu_2AlO_7$ appears to be a superposition of the spectra from sites with a large coupling constant, similar to that of $Sr_2YCu_{2.4}Al_{0.6}O_7$, and a small amount of intensity from sites with a smaller coupling. Ignoring the contribution of the component with the smaller coupling, comparison of the spectra for the different transitions gives a coupling constant of ≈9.7 MHz and an asymmetry parameter less that 0.15 for the broad component of $Sr_2YCu_2AlO_7$. The spectrum of $Sr_2YCu_{2.4}Al_{0.6}O_7$ corresponds to a slightly larger coupling constant and probably the same symmetry. Close examination of this spectrum shows that it too contains a small contribution from the narrower line. The spectrum of $Ba_2YCu_{2.8}Al_{0.2}O_7$ has a notably different line shape than the two strontium-based samples and does not exhibit the broadened cusps expected for a narrow distribution of site geometries, as is observed in the strontium samples.

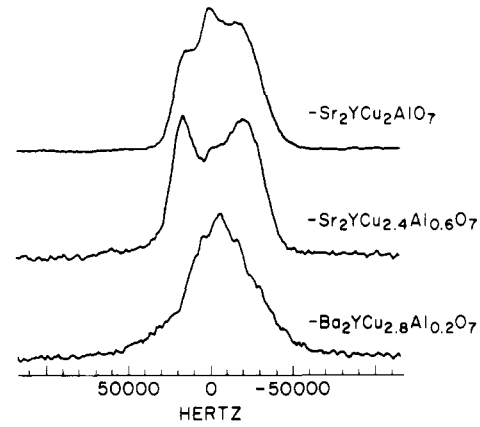

Figure 5. Room-temperature ^{27}Al spectra for the $^1/_2 \leftrightarrow -^1/_2$ NMR transition at 78.2 MHz for three aluminum-substituted cuprate perovskites.

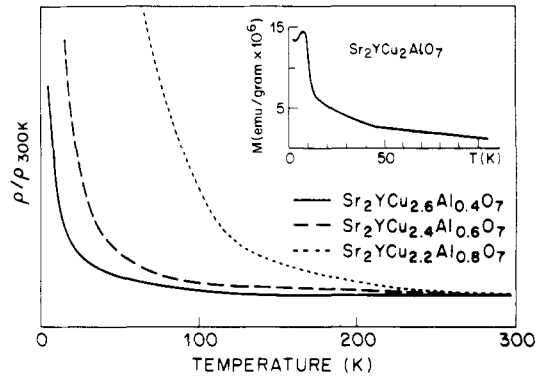

Figure 6. Normalized resistivity data for $Sr_2YCu_{3-x}Al_xO_7$, $x = 0.4$, 0.6, and 0.8. The inset shows magnetic behavior of $Sr_2YCu_2AlO_7$ at low temperatures.

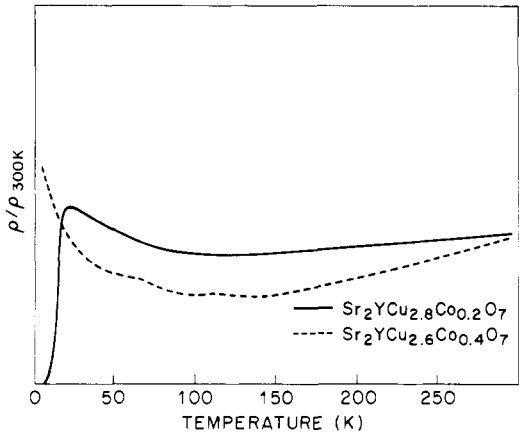

Figure 7. Normalized resistivity data for $Sr_2YCu_{2.8}Co_{0.2}O_7$ and $Sr_2YCu_{2.6}Co_{0.4}O_7$.

Physical Properties. The resistivity and magnetic susceptibility of several metal-stabilized Sr perovskites are given in Figures 6–8. A summary of room-temperature resistivities is given in Table V. In the case of Al, resistivity

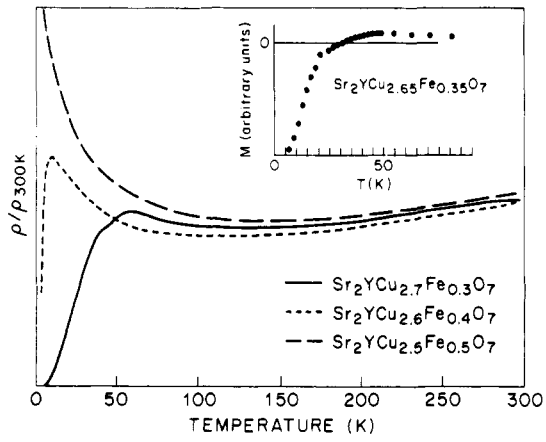

Figure 8. Normalized resistivity data for $Sr_2YCu_{3-x}Fe_xO_7$, x = 0.3, 0.4, and 0.5. The inset shows susceptibility data (0–100 K) for a sample with x = 0.35.

measurements show semiconducting of semimetallic behavior for all ceramic samples. Representative curves are shown in Figure 6. With the exception of the sample with x = 0.4, the room-temperature resistivity decreases with decreasing Al content as seen in Table V. The higher ρ observed for the x = 0.4 sample is probably due to impurities as this feature is observed with all metals close to the limits of phase stability. Magnetic measurements on aluminum-substituted samples that are electronically semiconducting show behavior consistent with antiferromagnetism. For $Sr_2YCu_2AlO_7$, a Néel temperature of 11 K was observed (Figure 6). For Fe- and Co-stabilized perovskites, samples with low levels of metal incorporation are superconducting, although for Co this is only the case is multiphase samples (Figures 7 and 8). At higher doping levels, superconductivity is lost and samples show semimetallic behavior. The highest T_c is observed for $Sr_2YCu_{2.7}Fe_{0.3}O_7$ with T_c^{onset} = 60 K and R = 0 at 10 K. Superconductivity in one Fe-substituted sample (x = 0.35) was confirmed by dc susceptibility measurements using a SQUID magnetometer but indicated only a 2% superconducting fraction (Figure 8). Such a small fraction could be attributable to an impurity phase. In all cases, these properties are reproducible in separate sample preparations.

Summary

Single-crystal diffraction shows that the metal atom positions in $Sr_2YCu_{3-x}M_xO_y$ are the same as in $Ba_2YCu_3O_7$ with the M ions substituting predominantly on the chain copper site. In $Ba_2YCu_{3-x}M_xO_y$ it has been proposed that the M ions replace the four-coordinate chain coppers while simultaneously introducing extra oxygen into the structure.[8] This results in a coordination number greater than four for the M ion and $y > 7$. It should be noted that full replacement of the chain Cu by an octahedral ion would lead to a stoichiometry $Ba_2YCu_2MO_8$. In $Ba_2YCu_2CoO_{7.4}$ the extra oxygen is coordinated to the Co ion.[8]

The behavior of the Sr system is quite different than the Ba system just described. For a given dopant level (e.g., 0.4) the a axis in the Sr system varies as Fe < Co < Al while in the Ba system Al < Co = Fe.[8] The latter order would be expected from a size effect since the Al ion is smaller than Fe or Co. The larger a axis in the case of Al and Co may also be caused by a difference in coordination geometry of these two ions. The degree of oxidation in the fully substituted compounds is also different for the Ba and Sr systems. For $Ba_2YCu_2MO_y$, $y > 7$ for M = Co and Fe while in the Sr system y = 7 for Co and Al and $y > 7$ only for Fe. The presence of only seven oxygens in both $Sr_2YCu_2AlO_7$ and $Sr_2YCu_2CoO_7$ suggests that both Al and Co are in a four-coordinate site. Oxide compounds containing both Al and Co ions in tetrahedral sites, including $LaSrCuAlO_5$[34] and Sr_2CoFeO_5,[35] are known. This coordination geometry is consistent with the TGA data that indicate that the oxygen atoms are tightly bound in these two phases. While the solid-state ^{27}Al NMR spectra cannot unambiguously identify a tetrahedral geometry, the spectra are characteristic of a site with a 3-fold or higher symmetry axis and rather large distortion of the structure along this axis. Since broadening of the spectra in these samples almost certainly results from variation of the quadrupole coupling parameters from site to site, $Sr_2YCu_{2.4}Al_{0.6}O_7$, which shows the least broadening, represents the most homogeneous crystal lattice. Results also suggest that $Ba_2YCu_{2.8}Al_{0.2}O_7$ contains Al in a variety of environments.

In the Fe-containing samples, the presence of more than seven oxygen atoms in highly substituted compounds would suggest a coordination number greater than four. A coordination number greater than four has been proposed for $Ba_2YCu_{3-x}M_xO_y$ compounds.[8] The different physical properties observed for different dopants may also be linked to changes in coordination geometry in the chain metal sites. In particular, the eventual loss of superconductivity in these systems may correspond to a rearrangement of the oxygen sublattice.

From the trends observed in room-temperature resistivities, it is clear that increasing the dopant concentration increases resistivity. Clearly, as the dopant level is reduced, the samples change from semiconducting to semimetallic or superconducting. Samples near the limit of phase stability, i.e., x = 0.4, have anomalously high resistivities, which is likely due to impurities not apparent in X-ray powder diffractograms. These trends suggest that a further reduction in dopant level, if possible, would further decrease ρ and enhance superconductivity.

In conclusion, we find that in the Sr–Y–Cu–O system, the perovskite phase is stabilized by metals that substitute on chain copper sites. Nickel or zinc, which are believed to substitute on plane sites in $Ba_2YCu_3O_7$,[8,21] do not stabilize the perovskite phase. Also, as Al, Fe, Co, and Pb all stabilize the perovskite phase, this stabilization is clearly not solely a size effect. The exact origin of this stabilization is still uncertain. Possible causes include structural changes or a change in the electronic structure. Further work is needed to fully understand this stabilization. We note the addition of another atom to the Sr–Y–Cu–O system greatly increases its complexity but provides for the occurrence of a structural arrangement conducive to superconductivity.

Acknowledgment. We thank R. B. van Dover, M. Stavola, D. Krol, and P. B. Littlewood for helpful discussions.

Supplementary Material Available: Listing of structure factor amplitudes (4 pages). Ordering information is given on any current masthead page.

(34) Wiley, J. B.; Markham, L. M.; Vaughey, J. T.; McCarthy, T. J.; Sabat, M.; Hwu, S.-J.; Song, S. N.; Ketterson, J. B.; Poeppelmeier, K. R., *Chemistry of High Temperature Superconductors II*; Nelson, D. L., George, T. F., Eds.; American Chemical Society: Washington, DC, 1988; p 304.

(35) Battle, P. D.; Gibb, T. C.; Lightfoot, P. *J. Solid State Chem.* **1988**, *76*, 334.